# Some Considerations for Measurements of Stresses in Rock Masses by the Use of Photoelastic Gages

By

Yoshiji NIWA*, Shoichi KOBAYASHI* and Ken-ichi HIRASHIMA*

(Received December 28, 1968)

In the first part of the present paper some considerations are made for several inherent problems to the stress measurements by the use of photoelastic gages such as the influences of the thickness of the binding agent, relative stiffness of the agent to the gage, the ratios of the depth of the bored hole to that of the gage and the ratios of the diameter of the overcoring to that of the bored hole.

In the second part applications of the photoelastic gages to the stress measurements in orthotropic rock masses are discussed.

## 1. Introduction

The first application of photoelastic technique to the measurements of stresses in rock masses was made about fifteen years ago[1], since then several improvements have been made[2].

In the first section of the present paper we shall discuss several problems inherent in the measurements of stresses by the use of photoelastic gages from the theoretical viewpoint. In the second section we shall describe the applications of photoelastic gages to the measurements of stresses in orthotropic rock masses.

## 2. Measurements of Stresses in Isotropic Elastic Masses

### 2.1. Some Considerations for Photoelastic Plugs (Inclusion Gages)

The applications of photoelastic plugs have been studied by several workers[3),4)], though there are some inherent problems in the application such as the influences of the binding agent, the bored hole, overcoring diameter and anisotropy of the rock masses. In this section the first three problems will be discussed and the last one will be discussed in the next section.

* Department of Civil Engineering

A. The influence of the thickness of the binding agent on isochromatics

There always exists a thin circular layer of the binding agent between the photoelastic plug and the rock masses. The influences of the thin layer on the measurement may not be disregarded when the elastic moduli of the plug and the binding agent are quite different, for example, glass plug and epoxy resin. In order to estimate the influences of the thickness of the layer on the isochromatics, let us consider a simple example as shown in Fig. 1. The uniform uniaxial load $p$ are applied at infinity in the $y$-direction. Isochromatics are obtained by some calculations with the following boundary conditions (denoted conditions (I)).

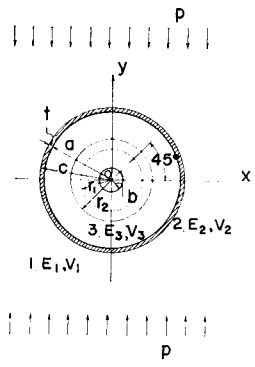


Fig. 1. Photoelastic gage and the coordinates (isotropic case).

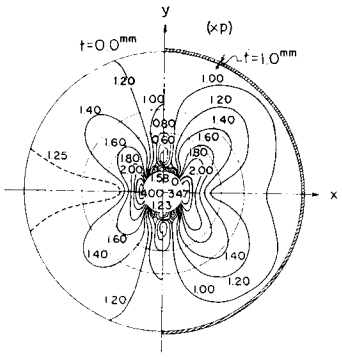


Fig. 2. Theoretical isochromatics in photoelastic plug taking into account of the thickness of binding agent (uniaxial load).

$$\sigma_r^{\,1} = \frac{p}{2}(1+\cos 2\theta), \quad \sigma_\theta^{\,1} = \frac{p}{2}(1-\cos 2\theta), \quad \tau_{r\theta}^{\,1} = -\frac{p}{2}\sin 2\theta \quad \text{at } r=\infty \quad (1)$$

$$\sigma_r^{\,1} = \sigma_r^{\,2}, \quad \tau_{r\theta}^{\,1} = \tau_{r\theta}^{\,2}, \quad u_r^{\,1} = u_r^{\,2}, \quad u_\theta^{\,1} = u_\theta^{\,2} \quad \text{at } r=c \quad (2)$$

$$\sigma_r^{\,2} = \sigma_r^{\,3}, \quad \tau_{r\theta}^{\,2} = \tau_{r\theta}^{\,3}, \quad u_r^{\,2} = u_r^{\,3}, \quad u_\theta^{\,2} = u_\theta^{\,3} \quad \text{at } r=a \quad (3)$$

$$\sigma_r^{\,3} = 0, \quad \tau_{r\theta}^{\,3} = 0 \quad \text{at } r=b \quad (6)$$

where $\sigma_r$, $\sigma_\theta$, $\tau_{r\theta}$, $u_r$ and $u_\theta$ are radial, tangential and shearing stresses and radial and tangetial displacements, respectively, and superscripts indicate the corresponding regions of Fig. 1.

As an example, theoretical isochromatics due to the uniaxial load are shown in the right-half of Fig. 2, where $E_1=2.1\times10^5$ kg/cm$^2$, $\nu_1=0.20$, $E_2=3.15\times10^4$ kg/cm$^2$, $\nu_2=0.36$, $E_3=6.3\times10^5$ kg/cm$^2$, $\nu_3=0.20$, $c=1.90$ cm, $a=1.80$ cm and $b=0.30$ cm. The left-half of Fig. 2 shows the theoretical isochromatics for the same conditions

(I) but $a=c$ *i.e.* the second thin layer is disregarded[3]. Although the general pattern of both isochromatics are alike many differences in the fringe orders are observed, especially in the neighborehood along the $y$-axis and on the inner radius of the plug. Therefore it is advisable to take into consideration the influences of the thickness of the binding agent, when the hard plug such as glass is used.

B. The influence of the ratio of the depth of the borehole to that of the plug

In the field application of the photoelastic plug, it is necessary to bore a considerably deep hole compared to the depth of the plug in order to avoid the disturbances of stresses due to stress concentrations at the bottom of the hole. In this situation the problem is, strictly speaking, three dimensional, which may be approximated in two ways. The first is to modify the solutions in plane stress with fictitious Young's modulus of the rock masses which is obtained by multiplying the true Young's modulus $E$ by the ratio of the depth of the hole to that of the plug. The second is based on the assumption that the plug is soft enough not to disturb the stresses in the mass. In this case the boundary conditions (denoted conditions (II)) on the outer boundary of the plug are quite simple and are equal to the displacements on the boundary of the Kirsch's solution for an infinite plate with a circular hole.

Examples of theoretical isochromatics due to uniaxial load with conditions (I), and (II) are shown in the left-half and the right-half of Fig. 3, respectively, where $E_1=3.0\times10^5$ kg/cm$^2$, $\nu_1=0.25$, $E_3=3.0\times10^4$ kg/cm$^2$, $\nu_3=0.36$, $b=0.15$ cm and $c=a=0.75$ cm i.e. $t=0$ in Fig. 1. As the ratio of the elastic modulus of the masses to that of the gage, i.e. $j=E_1/E_3$, decreases, the difference between the iso-

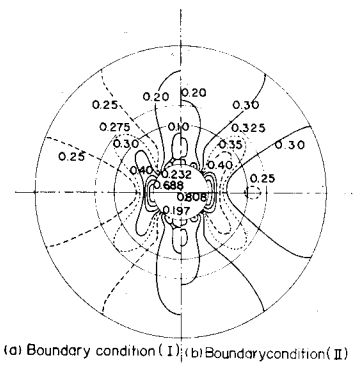


Fig. 3. Theoretical isochromatics in photoelastic plug due to boundary conditions (I) and (II) (uniaxial load).

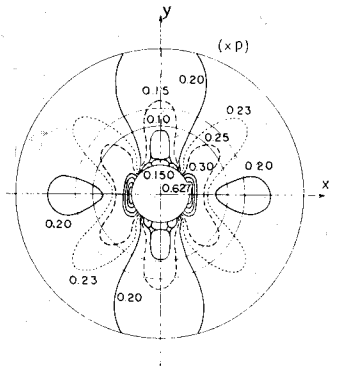


Fig. 4. Theoretical isochromatics in photoelastic plug for the case of overcoring at $r=3a$ (uniaxial load).

chromatics increases. For $j=70$, for example, the difference is at most 2.5 percent though for $j=10$, it is about 16 percent.

The actual state of stresses in the mass may lie between both estimations and probably closer to the estimation by the method with the fictitious Young's modulus.

C. The influence of overcoring

Large scale overcoring is sometimes impracticable in the field application, since in addition to the economical reason many fissures and cracks always develope in the rock masses. Two solutions may be useful. One is to reduce the ratio of the radius of overcoring to that of the photoelastic gage. Another is to use the small-sized photoelastic gage. In the first method some corrections must be made for the observed isochromatics. The corrected stresses are calculated with modified boundary conditions on the overcoring radius $r=r_0$,

$$\sigma_r^{\,1} = \sigma_r^{\,*}, \quad \tau_{r\theta}^{\,1} = \tau_{r\theta}^{\,*} \qquad \text{at} \quad r = r_0 \tag{5}$$

where $\sigma_r^{\,*}$ and $\tau_{r\theta}^{\,*}$ are stresses at $r=r_0$ in the Kirsch's solution.

The theretical isochromatics for $a/b=5.0$ and $r_0/a=3.0$ are shown in Fig. 4, where $E_1=3.0\times10^5$ kg/cm$^2$, $\nu_1=0.25$, $E_3=3.0\times10^4$ kg/cm$^2$ and $\nu_3=0.36$. In this example the reduction of fringe orders from those overcored at infinity (the left-half of Fig. 3) is at most 12 percent. Thus if we overcore with the radius more than four or five times the radius of the gage, no serious errors will be introduced.

Concerning a small-sized photoelastic gage authors tried photoelastic plugs with radii 0.6 cm$\sim$1.0 cm in "field" measurements of initial stresses. The isochro-

Fig. 5. Overcoring in the field using an electric hand drill.

matics are slightly affected by the irregularities of rock masses. This shortcoming, however, may be overcome by many-point measurements. The overcoring process is very simplified and can be easily carried out by an electric hand drill as shown in Fig. 5.

## 2.2 Applications of Birefringent Coating Gage

Stress measurement by the use of birefringent coating gage was first developed by Oppel[5] and has been recently applied to rock by Hawkes and Moxon[6]. In the field applications two problems arise. One is the ratio of the outer radius to the inner radius of the gage. Another is the low sensitivety of the photoelastic material.

A. Theoretical isochromatics

Let $a$ and $b$ the outer and inner radii of the birefringent coating gage and the gage be bonded at the outer radius $a$ to the mass. The displacements of the mass at $r=a$ are transmitted to the gage. Thus the isochromatics are of course influenced by the ratio $a/b$, although the Kirsch's solution is used in the references (5, 6). As an example, isochromatics by Kirsch's and exact solution under uniaxial load are compared in Fig. 6, where the ratio $a/b=5.0$ and the elastic constants are $E_1=3.0\times 10^5$ kg/cm$^2$, $\nu_1=0.25$, $E_3=3.0\times 10^4$ kg/cm$^2$ and $\nu_3=0.36$. Fig. 7 shows the relation between the difference of the principal stresses at some selected points on $r=\dfrac{(a-b)}{2}$ and the ratio of the load $q/p$ ($q$ is in the transverse direction to $p$). Considerable discrepancies between the Kirsch's solution and the exact one for $a/b=3.0$ are observed. The differences between isochromatics in the gage with

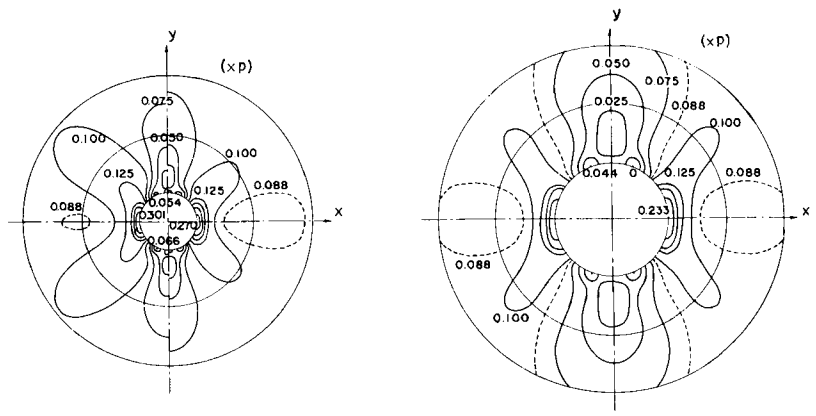


(a) The Kirsch's solution and the exact one ($a/b=5.0$).

(b) The exact solution ($a/b=3.0$).

Fig. 6. Theoretical isochromatics in birefringent coating gage (uniaxial load).

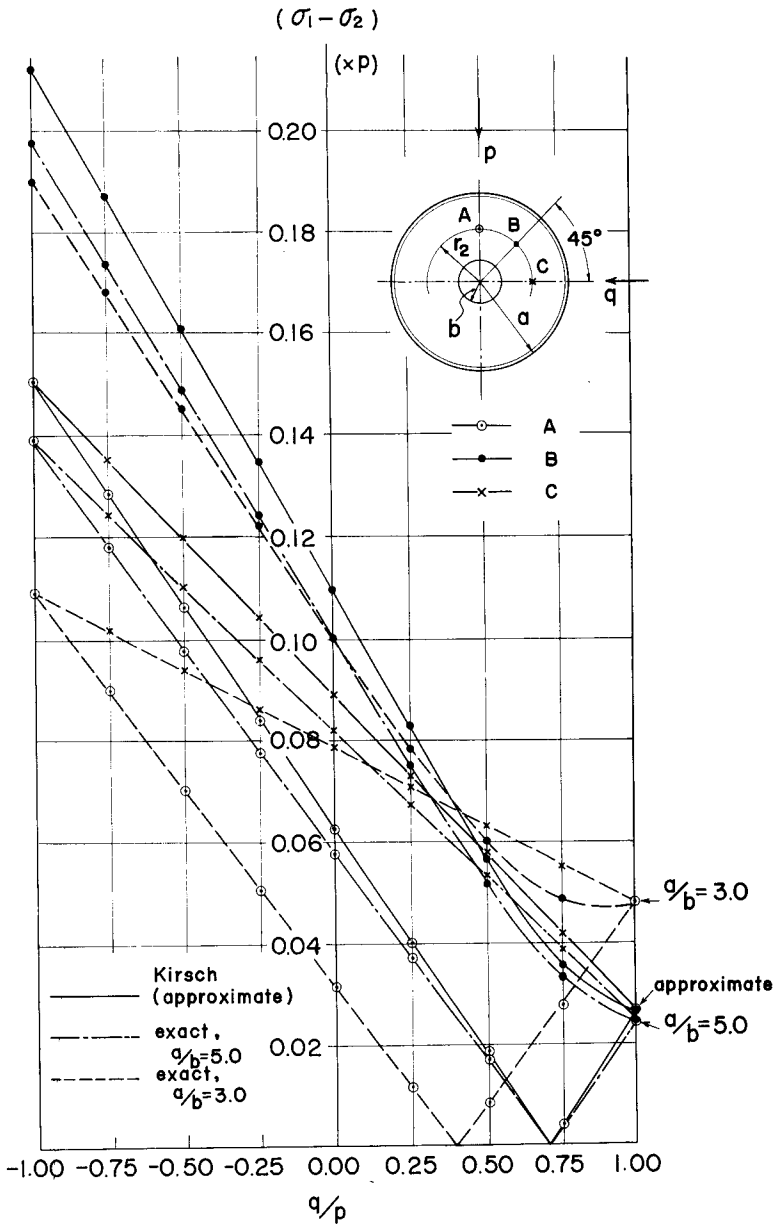


Fig. 7. Theoretical principal stress differences at points A, B and C versus principal load ratio $q/p$.

$a/b=3.0$ and those with $a/b=5.0$ are also observed in Figs. 6 and 8.

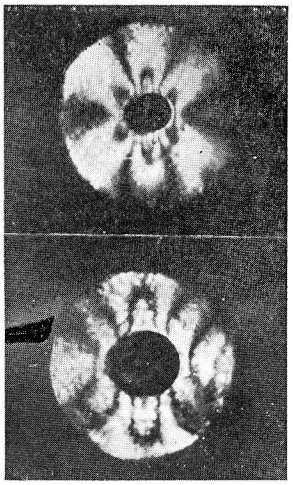

Fig. 8. Experimental isochromatics in birefringent coating gage (uniaxial load).

B. A new application of birefringent coating gage to stress relief method

The application of the birefringent coating gage to the measurements of the changes of stresses by Mathar method (drilling method) was first tried by Nishida[7]. This method, however, is not very accurate, since the strain sensitivity of the photoelastic material is not high enough. To improve this shortcoming, the authors tried a new method which also combines the stress-relief technique. The elastic mass to be measured is drilled to increase stress concentration and then

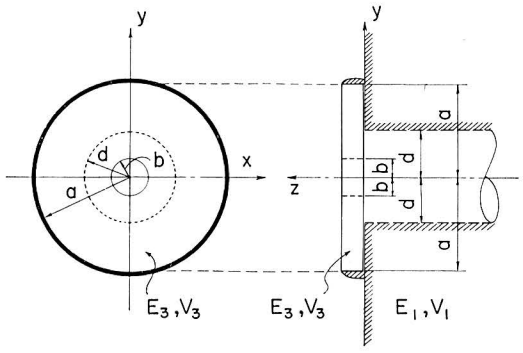


Fig. 9. Birefringent coating gage and the coordinates.

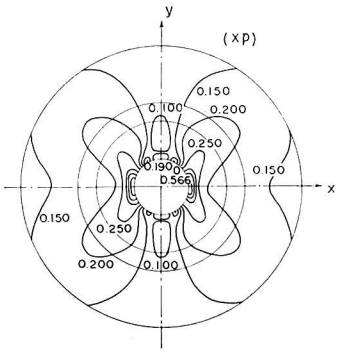


Fig. 10. Isochromatics in birefringent coating gage with $a/b=5.0$ and $d/a=2/3$ (uniaxial load).

birefringent coating gage is bonded concentrically with a hole along the outer radius to the mass as shown in Fig. 9. Finally stresses are released by concentric overcoring.

Fig. 10 shows an example of the theoretical isochromatics under uniaxial load with $a/b=5.0$ and $d/a=2/3$. As the radius of the hole increases, higher fringe in the gage appears. When the ratio $a/b=5.0$ and $d/a=0.84$, the present method leads to the same stress concentration as given by the photoelastic plug as shown Fig. 11.

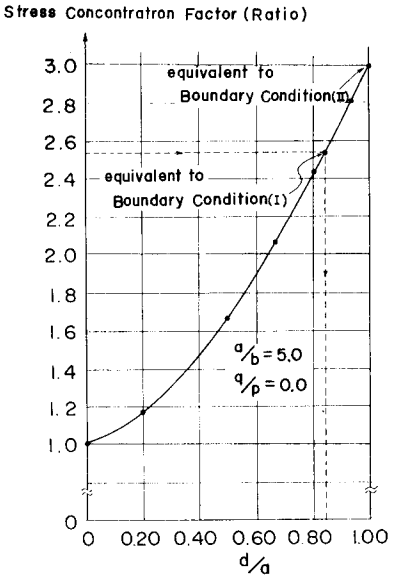


Fig. 11. The relations between stress concentration factors and $d/a$.

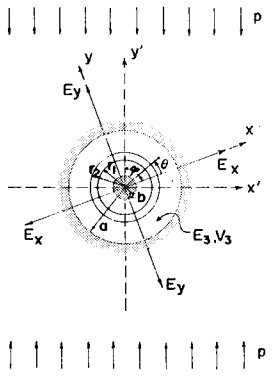


Fig. 12. Photoelastic gage and the coordinates (orthotropic case).

## 3. Measurements of Stresses in Orthotropic Elastic Masses

### 3.1 Isochromatics in the Photoelastic Plug

We shall consider a photoelastic plug placed in an orthotropic elastic body. Let the coordinate axis be in the principal directions of the elastic constants and the uniaxial load $p$ applied at infinity be inclined $\varphi$ from the reference coordinate axis $x$ as shown in Fig. 12. For the sake of simplicity, in this paper we assume the conditions (II) of the previous section. More elaborate treatment with conditions (I) has been given in reference (8).

Displacements on the hole surface of the orthotropic elastic body are given by

$$\left.\begin{aligned} u_r^1 &= -\frac{1}{2}pa\{(\alpha_1+\beta_1)+(\alpha_1-\beta_1)\cos 2\theta+(\alpha_2+\beta_2)\sin 2\theta\} \\ u_\theta^1 &= \frac{1}{2}pa\{(\alpha_2-\beta_2)+(\alpha_1-\beta_1)\sin 2\theta-(\alpha_2+\beta_2)\cos 2\theta\} \end{aligned}\right\} \quad (6)$$

where

$$\left.\begin{aligned} &\alpha_1 = a_{11}\{(1+\xi)\cos^2\varphi-\eta\sin^2\varphi\}, \quad \alpha_2 = \left\{a_{11}(\xi+\eta)+a_{12}+\frac{1}{2}a_{66}\right\}\sin\varphi\cos\varphi \\ &\beta_1 = a_{22}\left\{\left(1+\frac{\xi}{\eta}\right)\sin^2\varphi-\frac{1}{\eta}\cos^2\varphi\right\}, \quad \beta_2 = \left\{a_{22}\left(\frac{1+\xi}{\eta}\right)+a_{12}+\frac{1}{2}a_{66}\right\}\sin\varphi\cos\varphi \\ &\xi = \sqrt{\frac{2a_{12}+a_{66}}{a_{11}}+2\sqrt{\frac{a_{22}}{a_{12}}}}, \quad \eta = \sqrt{\frac{a_{22}}{a_{11}}}. \end{aligned}\right\} \quad (7)$$

The elastic constants $a_{11}$, $a_{12}$, $a_{22}$ and $a_{66}$ are related to the Young's modulus and the Poisson's ratio as follows:

$$a_{11} = \frac{1}{E_x}, \quad a_{22} = \frac{1}{E_y}, \quad a_{12} = -\frac{\nu_{xy}}{E_x} = -\frac{\nu_{yx}}{E_y}, \quad a_{66} = \frac{1}{G_{xy}} \qquad \text{in plane-stress}$$

$$a_{11} = \frac{1-\nu_{xz}\cdot\nu_{zx}}{E_x}, \quad a_{22} = \frac{1-\nu_{yz}\cdot\nu_{zy}}{E_y}, \quad a_{12} = -\frac{\nu_{xy}+\nu_{yz}\cdot\nu_{zy}}{E_x}, \quad a_{66} = \frac{1}{G_{xy}}$$

in plane-strain

Employing the conditions (II) as the boundary conditions, the stress function for the gage can be given by

$$\begin{aligned} \phi(r,\theta) = {} & A_0r^2+B_0\ln r+(A_2r^4+B_2r^{-2}+C_2r^2+D_2) \\ & \cos 2\theta+(A_2'r^4+B_2'r^{-2}+C_2'r^2+D_2')\sin 2\theta \end{aligned} \quad (8)$$

The unknown constants are determined by the boundary conditions (II).

Two examples of isochromatics are shown in Fig. 13 (b), where $E_3=3.0\times10^5$ kg/cm$^2$, $\nu_3=0.36$ for the gage and $E_x=E_1=3.0\times10^5$ kg/cm$^2$, $E_y=E_2=1.5\times10^5$ kg/cm$^2$ ($e=E_x/E_y=2.0$), $\nu_{xy}=0.25$ and $G_{xy}=1/(1/E_x+1/E_y+2\nu_{xy}/E_x)$ for the rock masses and $a/b=5.0$. Fig. 13 (a) shows the isochromatics for the same case as the above with conditions (I). These figures show that the principal directions of the fringe patterns do not coincide with the direction of the applied load $p$. The deviation angle $\delta$ from the direction of the applied load $p$ is a function of the ratio of the principal Young's modulii $e=E_x/E_y$, inclination angle $\varphi$ from the loading direction and the loading ratio $q/p$ in the biaxial states of stresses. As an example, the relations between $\delta$ and $\varphi$ with parameters $e$ under uniaxial load are shown in Fig. 14, assuming $E_x=3.0\times10^5$ kg/cm$^2$ and $\nu_{xy}=0.25$.

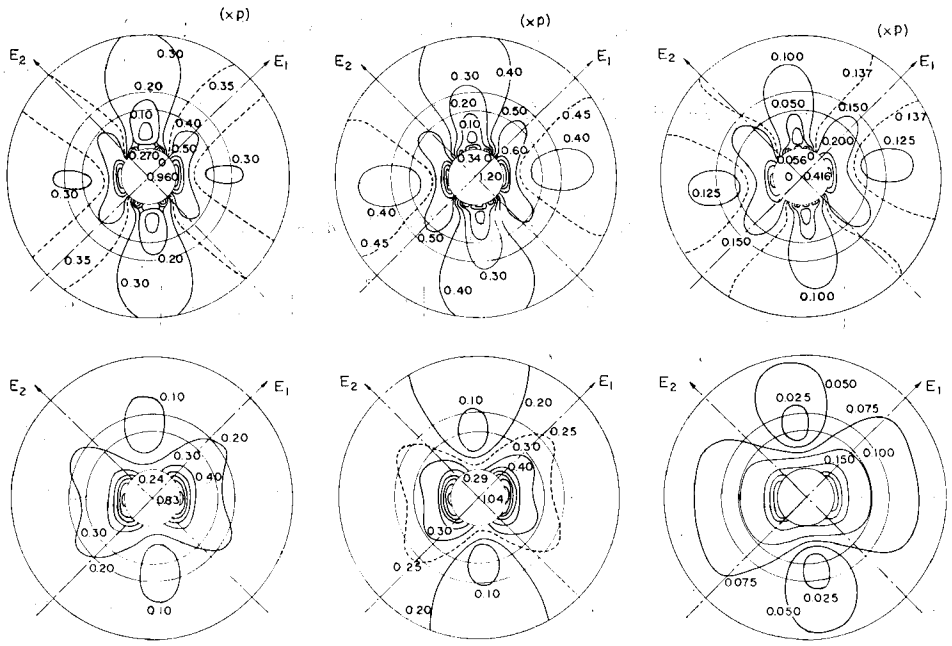


(a) Boundary conditions (I) (b) Boundary conditions (II) (c) Birefringent coating gage

Fig. 13. Theoretical isochromatics in photoelastic gage ($E_1/E_2=2.0$, $\varphi=45°$, $q/p=0.0$ and 0.50).

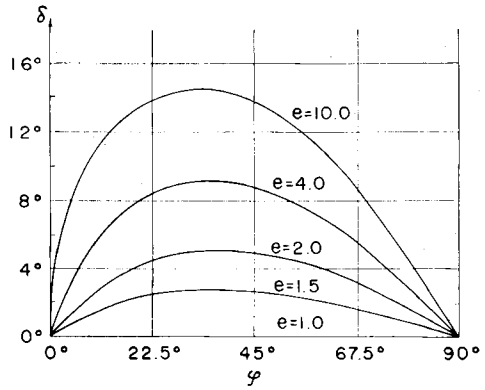


Fig. 14. The relations between deviation angles $\delta$ and the inclination angles $\varphi$ (boundary conditions (II)).

In order to verify the above mentioned theory, a small photoelastic gage made of diarylphtalate (DAP) resin with $a=0.75$ cm, $b=0.15$ cm and gage depth $d=0.20$ cm was bonded completely in an orthotropic plate made of epoxy resin with thin steel wires[10]. Fig. 15 shows iscochromatics when uniaxial load are applied from the direction $\varphi=45°$. The corresponding theoretical isochromatics are shown in Fig. 16. The agreement of both isochromatics is quite good.

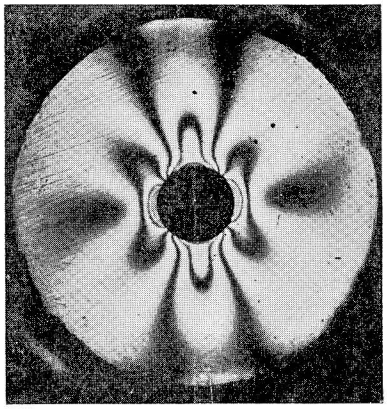

Fig. 15. Experimental isochromactis in photoelastic plug (uniaxial load, $E_1/E_2=4.0$, $\varphi=45°$).

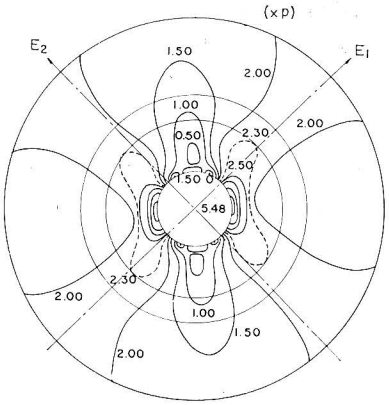


Fig. 16. Theoretical principal stress differences (uniaxial load, $E_1/E_2=4.0$, $\varphi=45°$).

### 3.2. Isochromatics in Birefringent Coating Gage.

Photoelastic birefringent coating gage can also be applied to an orthotropic elastic body. In this case the displacements along the outer radius $a$ are obtained from Eq. (6) with coefficients

$$\left.\begin{aligned} \alpha_1 &= a_{11}\cos^2\varphi + a_{12}\sin^2\varphi, \quad \alpha_2 = \frac{1}{2}a_{66}\sin\varphi\cos\varphi \\ \beta_1 &= a_{12}\cos^2\varphi + a_{22}\sin^2\varphi, \quad \beta_2 = \frac{1}{2}a_{66}\sin\varphi\cos\varphi \end{aligned}\right\} \tag{9}$$

Typical examples of isochromatics are shown in Fig. 11 (c) for the same elastic constants and sizes as in the previous example.

### 3.3 Determination of States of Stresses

From the isochromatics and the deviation angle $\delta$ in the photoelastic gage the principal stresses $p$ and $q$, and the inclination of the load $\varphi$ from the $E_x$-direction are determined as follows.

(i) Determine the elastic constants $E_x$, $E_y$, $\nu_{xy}$ and $G_{xy}$ of the orthotropic rock to be measured.

(ii) Determine the principal direction $\varphi'$ of the fringe pattern from the isochromatics. It is generally different from the inclination of the load $\varphi$ from the $E_x$-direction.

(iii) Using the deviation angle $\delta$ corresponding to $e=E_x/E_y$ and $\varphi$ (cf. Fig. 14) determines the true direction by $\varphi \fallingdotseq \varphi' - \delta$.

(iv) Calculate the theoretical isochromatics for appropriate load ratio $\omega=q/p$ and draw curves such as shown in Fig. 17.

(v) Obtain the ratio $k$ of the fringe order $n_{90}$ (at a point $\varphi-\theta=90°$ on $r=r_2$) to that $n_{45}$ (at a point $\varphi-\theta=45°$ on $r=r_1$), *i.e.* $k=n_{90}/n_{45}$, where $r_1=(a-b)/3$ and $r_2=(a-b)/2$. Estimate the load ratio $\omega=q/p$ from figures obtained from (iv).

(vi) Determine the load $p_i$ from the expression

$$p_i = \frac{1}{f_i} \cdot \frac{s}{d} n_i$$

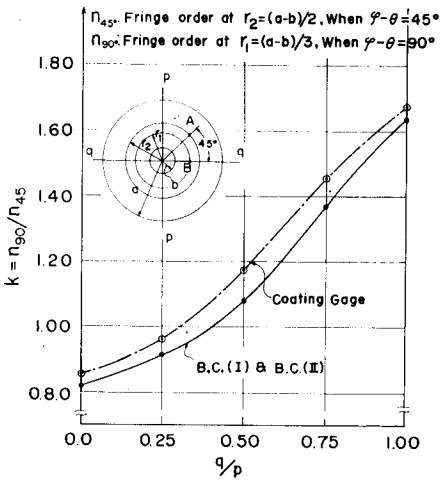


Fig. 17. Retlations betwen the load ratios $q/p$ and principal stress differences on the radius $(a-b)/3$ or $(a-b)/2$ ($E_x/E_y=2.0$, $\varphi=45°$ and boundary conditions (II)).

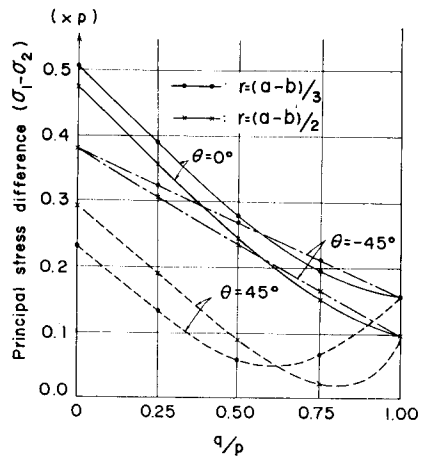


Fig. 18. Relations between the ratios $k=n_{90}/n_{45}$ and the load ratios $\omega=q/p$ ($E_x/E_y=2.0$, $\varphi=45°$)

where $n_i$ is the fringe order at point on $r=r_1$ or $r_2$ and $\varphi-\theta=0°$, 45° or 90°, $s$ is stress fringe value of the gage material, $d$ is the depth (optical pass) of the gage and $f_i$ is the differrence of principal stresses $(\sigma_1-\sigma_2)$ which correspond to known values of $\omega=q/p$ and $\theta$, whose relations are such as shown in Fig. 18, for example. Determine the most probable value $p$ from $p_i$ obtained at several points in the gage.

(vii) Determine the load $q$ by

$$q = \omega \cdot p$$

The above mentioned procedures can be also applied for the stress measurement of isotropic rock by taking $\varphi=0$.

## 4. Conclusions

Investigations so far carried out into the problems and techniques for stress measurements in rock masses by the use of photoelastic gages are done and the following may be concluded:

(1) When the photoelastic plug is used, the influences of the thickness of the binding agent on the isochromatics must be taken into account, especially when the hard plug is used.

(2) In field applications the depth of the bored hole is many times that of the photoelastic plug. To obtain the correct estimation of the working stresses the isochromatics of the plug must be interpreted by taking into accout the ratios of the depth of the bored hole to that of the plug.

(3) The influences of the overcoring on isochromatics are not very serious, if the ratios of the radius of the overcoring to that of the photoelastic gage are more than four.

(4) The stress measurement techniques by the use of birefringent coating gages so far proposed by applying the Kirsch's solution are approximate. The exact solution must be derived by taking into consideration the ratios of the outer radius to the inner radius of the gage. In order to overcome the low sensitivity of the birefringent coating gage the authors proposed a new method which is to bond the gage along the outer radius to masses concentrically with the hole bored beforehand and then to release stresses by concentric overcoring.

(5) The stress measurement techniques by the use of photoelastic gages are also applicable to orthotropic masses.

(6) In order to simplyfy the process and to be applicable to fissured rocks in-situ stress measurements, small sized photoelastic plugs with radii 0.6$\sim$1.0 cm were used. Although the isochromatics are slightly affected by the irregularities of rock masses, many-point measurements will overcome the shortcoming.

### References

1) Y. Hiramatsu, Y. Niwa and Y. Oka; Tech. Reps. of Eng. Res. Inst., Kyoto Univ., Vol. **7**, No. 3, March (1957), pp. 1–15
2) Y. Hiramatsu, Y. Niwa and Y. Oka; Mem. Faculty of Eng., Kyoto Univ., Vol. **29**, Jan. (1967), pp. 58–75
3) Ibid. 1), 2)
4) A. Roberts, I. Hawkes, F.T. Williams and R.K. Dhir; Intern. Journ. of Rock Mech. and Min. Sci., Vol. **1**, (1964), pp. 65–73
5) G.U. Oppel; Exp. Mech., Vol. **18**, (1961), pp. 65–73

6) I. Hawkes and S. Moxon; Intern. Journ. of Rock Mech. and Min. Sci., Vol. **2**, (1965), pp. 405–419
7) M. Nishida; Oyo-Butsuri, Vol. **31**, (1962), pp. 823–829 (in Japanese)
M. Nishida and H. Takabayashi; Proc. 13th Japan Nat. Congr. for Appl. Mech., (1963), pp. 108–113
8) Y. Niwa, S. Kobayashi and K. Hirashima; Preprint presented to Intern. Symp. on Rock Mech., Madrid (1968)
9) G. Sonntag; Der Bauingenieur, Band **33**, Heft 8 (1958), S. 287–294
10) Y. Niwa and T. Kawamoto; Trans. Japan Soc. Civil Eng., Vol. **83**, (1962), pp. 1–10 (in Japanese)